Applied and Computational Mathematics
2025; 14(1): 1-11
http://www.sciencepublishinggroup.com/j/acm
doi: 10.11648/j.acm.20251401.11
ISSN: 2328-5605 (Print); ISSN: 2328-5613 (Online)

Maximum Discharge of Lateral Pipes in Sewage Flow

Reuben Wambugu Mwangi, Mathew Ngugi Kinyanjui, Phineas Roy Kiogora*

Department of Pure and Applied Mathematics, Jomo Kenyatta University of Agriculture and Technology, Nairobi, Kenya

Email address:

reubenah.mwangi100@gmail.com (Reuben Wambugu Mwangi), mathewkiny@jkuat.ac.ke (Mathew Ngugi Kinyanjui), Prkiogora@fsc.jkuat.ac.ke (Phineas Roy Kiogora)
*Corresponding author

To cite this article:

Reuben Wambugu Mwangi, Mathew Ngugi Kinyanjui, Phineas Roy Kiogora. (2024). Maximum Discharge of Lateral Pipes in Sewage Flow. *Applied and Computational Mathematics, 14*(1), 1-11. https://doi.org/10.11648/j.acm.20251401.11

Received: 20 November 2024; **Accepted:** 3 December 2024; **Published:** 2 January 2025

Abstract: Rapid growth and population increase in urban centers has led to unplanned and rushed construction of buildings and amenities. This has led to poor development of sewer intakes from the buildings to the main sewer line. Therefore sewer blockage and low velocity of the sludge have been witnessed. The aim of this study is to investigate on how to achieve a maximum discharge of the lateral pipes into the main sewer line both from buildings and service (streets) sewer lines. This is achieved when sewerage system discharge is determined by the size of the sewer pipe used, effective inflow into the main sewer (linkages), slope (excavation depth) and distance between manhole. The governing equations for the flow are equation of continuity, momentum equations, energy equation and concentration equation. The nonlinear partial differential equations are transformed to ordinary differential equations, then solved numerically using the Collocation Method using an inbuilt MATLAB library known as Bvp4c. Velocity profiles, temperature profiles and the concentration profiles obtained are analyzed and discussed on how they affect the maximum discharge of sewer flow. Flow parameters are varied and their effect on the flow variables are determined and discussed. This study has remarkable applications in designing of the water, sanitation and sewer systems. This will reduce outbreak of diseases such as cholera, typhoid and enhance clean water and environment.

Keywords: Lateral Discharge, Sewage, Thermophoresis, Non-Newtonian Fluid, Viscous Fluid Flow

1. Introduction

Increased population growth in urban centers has led to rapid development of infrastructures. Rushed and unplanned connections of the lateral sewer pipes without considering maximum discharge into the main sewer pipe from this buildings and streets lines have been witnessed. Sewerage, water and sanitation systems has been immensely affected leading to shotage of clean water and outbreak of diarrheal diseases and Skin infections. The latter has been caused by overflow of sewage sludge within the lateral connections to the environment due minimal discharge into the main sewer line and due to the haste connections of this lateral sewer pipes to the main sewer pipe. It is imperative to study how to achieve a maximum discharge of lateral sewer connections into the main stream to enable effective sludge flow throughout the system and also to allow efficient sludge flow thereby reducing bursting of pipes as a result of clogging. It is also key to study blockage of pipes to allow proper maintenance of sewer lines.

J. W. Thiong'o investigated on open rectangular and triangular channel flows. She aimed to identify which of the open rectangular and triangular channels has a higher hydraulic efficiency. The approximate solution of the partial differential equations governing the flow is obtained numerically through the application of the finite difference method. The results showed that the flow's velocity increases with depth and reaches its maximum just below the free surface. Additionally, an increase in the energy coefficient, top-width, and channel slope all result in higher flow velocities, whereas an increase in the roughness coefficient causes lower flow velocities. Finally, she discovered that an open rectangular channel outperforms an open triangular channel in terms of hydraulic efficiency for a fixed flow depth and width. [1]

P. K. Marangu et al. researched on simulating fluid flow in an open channel with a segment base and a trapezoidal

cross-section. He considered uniform, steady open channel flow where the finite difference approximation method was used to solve the partial differential equations of the governing equations. Focused on how the flow velocity is affected by the channel radius, cross section area, flow depth, and manning coefficient. The results showed that a drop in flow velocity is caused by an increase in the flow's cross section area. Moreover, a drop in flow velocity is caused by an increase in the roughness coefficient and a decrease in the flows cross section area and channel radius. Moreover, velocity rises with increasing flow depth. [2]

S. M. Karimi studied fluid flow in open rectangular channels with lateral inflow. He considered an incompressible, Newtonian fluid flow taking into account how the crosssectional area, velocity, length, and angle which range from zero to ninety degrees affect the flow velocity in the primary open rectangular channel. The finite difference method is used to numerically derive an approximate solution of the partial differential equations governing the flow. The results showed that discharge is directly proportional to the flow velocity, therefore a rise in flow velocity corresponds to an increase in discharge, and vice versa. [3]

M. Rubinato et al. studied circular inlets that facilitate the exchange of surface to sewer flow during urban flooding conditions. He considered a large number of experimental datasets representing surface to sewer flow exchange through a circular inlet under steady state settings using ten various inlet grate designs using a physical scale model. The flow depths that were measured experimentally and those that were numerically modeled accord, however there are more differences at higher flow exchange rates. Using calibrated 2D numerical finite difference technique (FDM) he described observed surface flow depths in the region of the inlet structure, and he was able to derive acceptable weir/orifice discharge coefficients applicable to describe exchange flows. [4]

D. Singh et al. investigated a gravity fed sewer line's optimal design using linear programming. In his model he considered the separation between two successive manholes and the sewage line's slope, which maintains the self cleaning velocity as the optimization model's constraints. He took into account those available diameters that meet the self cleaning velocity constraint and removed nonlinearity caused by the pipe size. The results showed that, the model determines the least value of the overall cost of the entire sewer line where the pipe widths and slope between various manholes are chosen to maintain the self cleaning velocity. Also reduce the overall cost of the sewer line, which includes the costs of the pipeline, excavation, and manhole, a linear programming model is created. [5]

N. Ayub et al. carried a case study for Mbale Municipality using computational fluid dynamics (CFD) to create a model that would improve sewage flow through pipemanhole drainage systems. He considered an incompressible fluid , turbulent fluid flow and a sewer which is a mixture flow of air and water. The results showed that there is a reasonable degree of agreement between the pressure drop, liquid velocity numbers, and flow pattern behavior. Also most efficient way to optimize a sewer network system for Mbale Municipality conditions is to take into account the sewer diameters, slope gradients for optimal sewer design, minimum and maximum sewer velocities in the range of 0.67 m/s to 5.5 m/s, respectively, and increasing the number of sewer network connections of residential, municipal, and industrial buildings. [6]

B. Huang et al. did an experimental study of geysers through a vent pipe connected to flowing sewers . Studied on impact of geysers of air-water mixtures in urban drainage systems. They found out that terminal velocity of a rising air where gas gravity acceration applies also effects on large air pockets and water columns that undergoes mass loss due to a counter-current water films that around the pipe walls. [7]

E. J. Noah et al. did a case study of Tororo Municipality in eastern Uganda where he studied how to optimize municipal sewage networks using computational dynamics. [8]

He considered an incompressible fluid, isothermal fluid and immiscible fluid and the body force added was Continuum surface force (CSF). After simulating a two-phase flow of sewage and air, he came to the conclusion that increasing the number of household sewer lateral network connections and modifying sewer diameters and slope gradients are the best ways to optimize a sewer network system.

J. Ebelait et al. used computational fluid dynamics to describe linkage leakage in sewage pipes via porous surfaces when there is just one leak. He considered a compressible fluid and used Ansys Fluent to obtain fluid simulations, based on the standard k-e model under steady-state conditions. The results showed that the pressure at the leak point rises with increasing outlet pressures, while the velocity at the leak point increases with increasing entrance velocity. Nevertheless, with higher inlet velocities, there is no appreciable shift in the sewage flow rate. Therefore, monitoring these fields is an essential tool for locating leaks since disturbances along the pipeline affect the pressure and velocity fields both before and after leaking. [9]

A. C. Chirchir studied the impact of two lateral inflow channels on discharge through the main channel. He considered a rectangular open channel and focused on the effects of cross-sectional area, length of two lateral inflow channels, and angles that vary directly proportionately to each other for two lateral inflow channels from zero to ninety degrees on the main channel's flow rate. By using the finite difference approach, the approximate solution of the partial differential equations regulating the flow is solved numerically. The results showed that the main channel's flow velocity is increased by a decrease in the length of the lateral inflow channels and an increase in the cross-sectional area of the lateral inflow channels. Additionally, the main channel's flow velocity is increased by sloped lateral inflow channels at 450 compared to 600 and 720, while the main channel's flow velocity remains constant at 900. [10]

The purpose of this study is to mathematically model and examine a sewer system in order to determine how to maximize the discharge from its lateral sewer connections (pipes) into the main stream to allow efficient sludge flow

throughout the system. Similarly investigating more on causes of deposition and clogging of sewer lateral pipes due to poor connections, slope and angles of the pipes, thus studying how flow of particles(contaminants) in the sewer systems cannot cause deposition and clogging. This study will help in reduction of environmental pollution, an increase in sanitation and an increase of clean water.

2. Mathematical Formulation

The sewer pipe is parallel to the terrain as shown in figure 1 where the flow is purely radial and the pipe is assumed to be fully-filled and the flow is two-dimensional along r and θ.

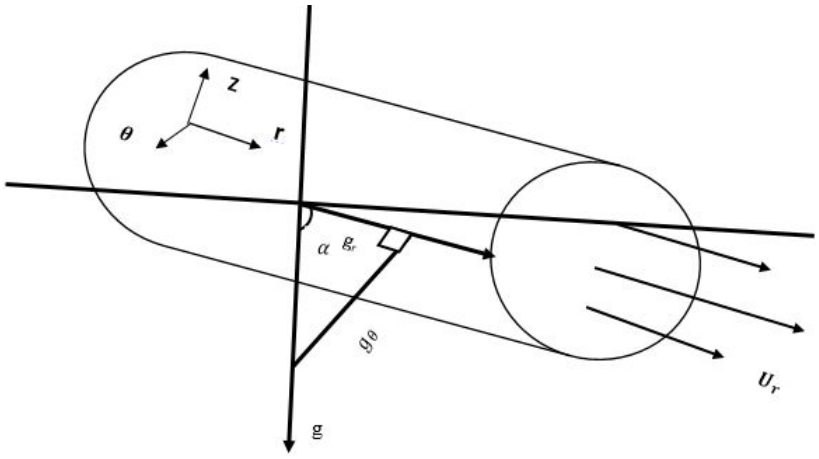

Figure 1. *Geometry of the problem.*

The sewage matter consider is water plus contaminants which makes the sludge, where this fluid is incompressible and the fluid flows is laminar where no-slip condition is satisfied and thermophoresis causes motion of this very fluid.

2.1. Governing Equations

The fundamental equations governing the sewer fluid flow are the equation of continuity, the momentum equations, the energy equation and the concentration equation.

2.1.1. Equation of Continuity

$$\frac{\partial \rho}{\partial t} + \frac{1}{r}\frac{\partial (\rho r u_r)}{\partial r} + \frac{1}{r}\frac{\partial (\rho u_\theta)}{\partial \theta} + \frac{\partial (\rho u_z)}{\partial z} = 0 \tag{1}$$

$$\frac{1}{r}\frac{\partial (r u_r)}{\partial r} = 0 \tag{2}$$

Equation (2) represents the equation of continuity in cylindrical coordinates for a two-dimensional unsteady, laminar flow of an incompressible fluid whose motion is purely radial.

2.1.2. Equation of Conservation of Momentum Along r

$$\rho\left(\frac{\partial u_r}{\partial t} + u_r\frac{\partial u_r}{\partial r} + \frac{u_\theta}{r}\frac{\partial u_r}{\partial \theta} + u_z\frac{\partial u_r}{\partial z} - \frac{u_\theta^2}{r}\right) = -\frac{\partial p}{\partial r} + \mu\left[\frac{1}{r}\frac{\partial}{\partial r}\left(r\frac{\partial u_r}{\partial r}\right) + \frac{1}{r^2}\frac{\partial^2 u_r}{\partial \theta^2} + \frac{\partial^2 u_r}{\partial z^2} - \frac{2}{r^2}\frac{\partial u_\theta}{\partial \theta} - \frac{u_r}{r^2}\right] + F_r \tag{3}$$

2.1.3. Equation of Motion Along θ

$$\rho\left(\frac{\partial u_\theta}{\partial t} + u_r\frac{\partial u_\theta}{\partial r} + \frac{u_\theta}{r}\frac{\partial u_\theta}{\partial \theta} + u_z\frac{\partial u_\theta}{\partial z} + \frac{u_r u_\theta}{r}\right) = -\frac{1}{r}\frac{\partial p}{\partial \theta} + \mu\left[\frac{1}{r}\frac{\partial}{\partial r}\left(r\frac{\partial u_\theta}{\partial r}\right) + \frac{1}{r^2}\frac{\partial^2 u_\theta}{\partial \theta^2} + \frac{\partial^2 u_\theta}{\partial z^2}\right] + \mu\left[\frac{2}{r^2}\frac{\partial u_r}{\partial \theta} - \frac{u_\theta}{r^2}\right] + \rho g_\theta \tag{4}$$

In this study gravitational forces are the forces driving the flow. Therefore considering that $F_r = \rho g_r$. Using Boussinesq approximation where $\rho(T, C)$, then $F_r = (\rho(T, C))\, g_r$.

The flow is caused by free convection, the pipe is tilted at an angle α ,where gravitation force affects the motion along the radial direction. This implies that:

$$g_r = gcos\alpha \tag{5}$$

T. M. Shih [11] defines bouyancy force (F_B) as: $F_B = g_r \Delta\rho$ Alan(1967) defined volume expansion coefficient β as a function of density (ρ) and Temperature (T).

$$F_B = \beta\,(T - T_\infty)\, g_r \tag{6}$$

Similarly the buoyancy forces due to concentration can be written as,

$$F_B = \beta\,(C - C_\infty)\,(gcos\alpha) \tag{7}$$

The flow is 2-D along (r,θ) and is purely radial (that is u_θ = 0 and u_z = 0). On differentiating the equation of continuity with respect to r and with respect to θ, using that the momentum equation along r direction reduces to:

$$\rho\left(\frac{\partial u_r}{\partial t} + u_r\frac{\partial u_r}{\partial r}\right) = -\frac{\partial p}{\partial r} + \mu\left[\frac{1}{r^2}\frac{\partial^2 u_r}{\partial\theta^2}\right] + \beta\,(T - T_\infty)\,(gcos\alpha) + \beta\,(C - C_\infty)\,(gcos\alpha) \tag{8}$$

and the momentum equation reduces to the following in θ directions:

$$0 = -\frac{1}{\rho r}\frac{\partial p}{\partial\theta} + \frac{\mu}{\rho}\left[\frac{2}{r^2}\frac{\partial u_r}{\partial\theta}\right] + \frac{\beta}{\rho}\,(T - T_\infty)\,(gsin\alpha) + \frac{\beta}{\rho}\,(C - C_\infty)\,(gsin\alpha) \tag{9}$$

Eliminating the pressure term p, by differentiating equation (8) with respect to θ and equation (9) with respect to r , and equating them we get the equation of motion for an unsteady, laminar, two dimensional flow of an incompressible fluid whose motion is purely radial as.

$$\begin{aligned}\frac{\partial^2 u_r}{\partial\theta\partial t} = {} & \frac{\mu}{\rho}\left[\frac{1}{r^2}\frac{\partial^3 u_r}{\partial\theta^3} + \frac{2}{r^2}\frac{\partial u_r}{\partial\theta} - \frac{2}{r}\frac{\partial^2 u_r}{\partial r\partial\theta}\right] - \frac{\partial u_r}{\partial\theta}\frac{\partial u_r}{\partial r} - u_r\frac{\partial^2 u_r}{\partial r\partial\theta} + \frac{\beta g_r}{\rho}\frac{\partial}{\partial\theta}\,(T - T_\infty) + \frac{\beta g_r}{\rho}\frac{\partial}{\partial\theta}\,(C - C_\infty) \\ & - \frac{\beta g_\theta}{\rho}\left[(T - T_\infty) + \frac{\partial}{\partial r}\,(T - T_\infty)\, r\right] - \frac{\beta g_\theta}{\rho}\left[(C - C_\infty) + \frac{\partial}{\partial r}\,(C - C_\infty)\, r\right]\end{aligned} \tag{10}$$

2.1.4. Equation of Energy

$$\rho c_p\left[\frac{\partial T}{\partial t} + u_r\frac{\partial T}{\partial r} + \frac{u_\theta}{r}\frac{\partial T}{\partial\theta} + u_z\frac{\partial T}{\partial z}\right] = \rho q_g + \Phi + \alpha\left[\frac{1}{r}\frac{\partial}{\partial r}\left(r\frac{\partial T}{\partial r}\right) + \frac{1}{r^2}\frac{\partial^2 T}{\partial\theta^2} + \frac{\partial^2 T}{\partial z^2}\right] \tag{11}$$

Where,

$$\begin{aligned}\Phi = {} & 2\mu\left[\left(\frac{\partial u_r}{\partial r}\right)^2 + \left(\frac{1}{r}\frac{\partial u_\theta}{\partial\theta} + \frac{u_r}{r}\right)^2 + \left(\frac{\partial u_z}{\partial z}\right)^2\right] \\ & + \mu\left[\left(\frac{1}{r}\frac{\partial u_r}{\partial\theta} + \frac{\partial u_\theta}{\partial r} - \frac{u_\theta}{r}\right)^2 + \left(\frac{\partial u_\theta}{\partial z} + \frac{1}{r}\frac{\partial u_z}{\partial\theta}\right)^2 + \left(\frac{\partial u_z}{\partial r} + \frac{\partial u_r}{\partial z}\right)^2\right]\end{aligned} \tag{12}$$

The fluid flow is purely radial, dividing through by ρc_p and making $\frac{\partial T}{\partial t}$ the subject:

$$\frac{\partial T}{\partial t} = \frac{(g_r)}{c_p} + \frac{\mu}{\rho c_p}\left[2\left(\frac{\partial u_r}{\partial r}\right)^2 + 2\left(\frac{u_r}{r}\right)^2 + \left(\frac{1}{r}\frac{\partial u_r}{\partial\theta}\right)^2\right] + \frac{\alpha}{\rho c_p}\left[\frac{1}{r}\frac{\partial T}{\partial r} + \frac{\partial^2 T}{\partial r^2} + \frac{1}{r^2}\frac{\partial^2 T}{\partial\theta^2}\right] - u_r\frac{\partial T}{\partial r} \tag{13}$$

The energy equation of the study is equation(13) , where q_g gravitation force, Φ viscous dissipation rate,T - temperature,c_p specific heat at constant pressure, $\frac{\alpha}{\rho c_p}$ thermal diffusivity and μ dynamic viscosity.

2.1.5. Concentration Equation

$$\frac{\partial C}{\partial t}+u_r\frac{\partial C}{\partial r}+\frac{u_\theta}{r}\frac{\partial C}{\partial \theta}+u_z\frac{\partial C}{\partial z}=D\left(\frac{1}{r}\frac{\partial}{\partial r}\left(r\frac{\partial C}{\partial r}\right)+\frac{1}{r^2}\frac{\partial^2 C}{\partial \theta^2}+\frac{\partial^2 C}{\partial z^2}\right)$$
$$+\frac{1}{r}\frac{\partial}{\partial r}(ru_{Tr}C)+\frac{1}{r}\frac{\partial}{\partial \theta}(u_{T\theta}C)+\frac{1}{r}\frac{\partial}{\partial \theta}(u_{TZ}C) \tag{14}$$

where $\frac{\partial C}{\partial t}$ is the temporal concentration, $\vec{\nabla}\left(C\overrightarrow{V}\right)$ represents the spatial concentration, D is the diffusion coefficient and u_T is the thermophoresis term.

Since the flow is radial:

$$\frac{\partial C}{\partial t}+u_r\frac{\partial C}{\partial r}=D\left(\frac{1}{r}\frac{\partial}{\partial r}\left(r\frac{\partial C}{\partial r}\right)+\frac{1}{r^2}\frac{\partial^2 C}{\partial \theta^2}\right)+\frac{1}{r}\frac{\partial}{\partial r}(ru_{Tr}C) \tag{15}$$

In this study thermophoresis in the θ direction and is considered because contaminants deposition occurs radially. [12] the thermophoresis velocity is defined by

$$u_T=-\frac{K_T}{T_r}\frac{\mu}{\rho}\frac{dT}{d\theta} \tag{16}$$

$\frac{dT}{dr}$ is the radial temperature gradient, K_T thermophoretic coefficient which ranges in value from 0.2 to 1.2 as indicated by [13]. Substituting equation(16) into equation(15) becomes:

$$\frac{\partial C}{\partial t}+u_r\frac{\partial C}{\partial r}=D\left(\frac{1}{r}\frac{\partial C}{\partial r}+\frac{\partial^2 C}{\partial r^2}+\frac{1}{r^2}\frac{\partial^2 C}{\partial \theta^2}\right)-\frac{\mu K_T}{\rho}\left[\frac{\partial^2 T}{\partial \theta^2}\frac{C}{T_r}-\frac{C}{T_r^2}\left(\frac{\partial T}{\partial \theta}\right)^2+\frac{1}{T_r}\frac{\partial T}{\partial \theta}\frac{\partial C}{\partial \theta}\right] \tag{17}$$

Equation (17) is the specific equation of concentration for unsteady laminar flow of an incompressible fluid whose motion is purely radial.

2.2. Similarity Transformation

The initial conditions are:

At the centre line at, $\theta=0$:

$$u_r=u_\infty,\frac{\partial u_r}{\partial \theta}=0,T=T_\infty,\frac{\partial T}{\partial \theta}=0,C=C_\infty,\frac{\partial C}{\partial \theta}=0 \tag{18}$$

On the wall $\theta=\alpha$:

$$\frac{\partial u_r}{\partial \theta}=-\gamma u(\theta),T=T_w,C=C_w \tag{19}$$

From [14] and [15], the following similarity transformations are used to transform the specific equations of the fluid flow model from partial differential equations to ordinary differential equations.

$$u_r=-\frac{Q}{r\delta^{m+1}}f(\theta) \tag{20}$$

$$T=\frac{(T_w-T_\infty)\,\omega}{\delta^{m+1}}+T_\infty \tag{21}$$

$$C=\frac{(C_\infty-C_w)\,\phi}{\delta^{m+1}}+C_w \tag{22}$$

Applying the transformations above into the equation of motion, energy equation and equation of concentration we have:

$$(m+1)\frac{\rho r^2}{\delta^{m+1}}\frac{d\delta}{dt}f^I(\theta)=-f^{III}(\theta)-2f^I(\theta)-2f^I(\theta)-2\frac{Q\rho}{\mu}\frac{1}{\delta^{m+1}}f(\theta)f^I(\theta)+\frac{\beta r^3 g_r}{\mu Q}\left[(T_f-T_\infty)\,\omega^I\right]$$
$$+\frac{\beta r^3 g_r}{\mu Q}\left[(C_\infty-C_w)\,\phi^I\right]-\frac{\beta r^3 g_\theta}{\mu Q}(T_f-T_\infty)\omega-\frac{\beta r^3 g_\theta}{\mu Q}\,(C_\infty-C_w)\,\phi \tag{23}$$

$$\frac{\alpha}{\rho c_p}\left[\omega^{II}\right]+\frac{(m+1)}{\delta^{m+1}}\frac{d\delta}{dt}r^2\omega+\frac{\mu Q^2}{\rho c_p r^2\delta^{(m+1)}\left(T_w-T_\infty\right)}\left[4\left(f(\theta)\right)^2+\left(f^I(\theta)\right)^2\right]+\frac{r^2\delta^{m+1}}{\left(T_w-T_\infty\right)}\frac{g_r}{c_p}=0 \tag{24}$$

$$\frac{(m+1)}{\delta^{m+1}}\frac{\rho}{\mu}\frac{d\delta}{dt}r^2\phi+\frac{\rho D}{\mu}\phi^{II}-\left[\frac{r^2K_T}{\omega+\frac{T_\infty\delta^{m+1}}{(T_w-T_\infty)}}\right]\omega^I\phi^I+\frac{r^2K_T}{\omega+\frac{T_\infty\delta^{m+1}}{(T_w-T_\infty)}}\left[\left(\phi+\frac{\left(C_f(\delta^{m+1})\right).}{(C_\infty-C_w)}\right)\frac{1}{\omega+\frac{T_\infty\delta^{m+1}}{(T_w-T_\infty)}}\right]\left(\omega^I\right)^2$$
$$-\frac{r^2K_T}{\omega+\frac{T_\infty\delta^{m+1}}{(T_w-T_\infty)}}\left[\left(\phi+\frac{\left(C_f(\delta^{m+1})\right).}{(C_\infty-C_w)}\right)\right]\omega^{II}=0 \tag{25}$$

On simplifying and introducing the dimensionless parameters

$$R_e=\frac{Q\rho}{\mu}=\frac{inertia forces}{viscous forces}, G_r(T)=\frac{\beta r^3 g_r}{\mu}\left(T_w-T_\infty\right)G_r(C)=\frac{\beta r^3 g_r}{\mu}\left(C_\infty-C_w\right)$$

$$Pr=\frac{\mu c_p}{\alpha}, Ec=\frac{Q^2}{c_p\left(T_w-T_\infty\right)}, S_C=\frac{\nu}{D}$$

$$N_t=\frac{T_\infty}{T_w-T_\infty}, N_C=\frac{C_\infty}{C_\infty-C_w}, \lambda=\frac{d\delta}{dt}\frac{\rho}{\mu}.$$

Where Reynolds number (Re), Thermal Grashof number($G_r(T)$), Mass Grashof number($G_r(C)$), Prandtl number (Pr), Eckert number (Ec), Schmidt number (Sc), Thermophoresis parameter (Nt), Concentration ratio(N_C) and Unsteadiness parameter (λ). Equations (23, 24, 25) reduces to:

$$(m+1)\frac{\lambda r^2}{\delta}f^I(\theta)=-f^{III}(\theta)-4f^I(\theta)-\frac{R_e}{\delta^{m+1}}f(\theta)f^I(\theta)+\frac{G_r(T)}{Q}\omega^I+\frac{G_r(C)}{Q}\phi^I-\frac{G_r(T)}{Q}\omega-\frac{G_r(C)}{Q}\phi \tag{26}$$

$$\frac{1}{Pr}(\omega^{II})+\frac{(m+1)r^2\lambda}{\delta^{m+1}}\omega+\frac{Ec}{r^2\delta^{m+1}}\left[4\left(f(\theta)\right)^2+\left(f^I(\theta)\right)^2\right]+\frac{r^2\delta^{m+1}}{\left(T_w-T_\infty\right)}\frac{g_r}{c_p}=0 \tag{27}$$

$$\frac{(m+1)}{\delta^{m+1}}\frac{\rho}{\mu}\lambda\phi+\frac{1}{S_C}\phi^{II}-\left[\frac{r^2K_T}{\omega+N_t\delta^{m+1}}\right]\omega^I\phi^I+\frac{r^2K_T}{\omega+N_t\delta^{m+1}}\left[\left(\phi+N_C(\delta^{m+1})\right)\frac{1}{\omega+N_t\delta^{m+1}}\right]\left(\omega^I\right)^2$$
$$-\frac{r^2K_T}{\omega+N_t\delta^{m+1}}\left[\left(\phi+N_C(\delta^{m+1})\right)\right]\omega^{II}=0 \tag{28}$$

The boundary conditions:
At the center line, $\theta=0$

$$f(0)=1, f^I(0)=0, \omega(0)=\delta^{m+1}, \phi(0)=\delta^{m+1} \tag{29}$$

At the walls, $\theta=\alpha$

$$f^I(\theta)=-\gamma f(\theta), \omega(\theta)=0, \phi(0)=0 \tag{30}$$

2.3. Methods of Solution

2.3.1. Collocation Method

This is the best method for solving BVPs and due to the geometry of the study it makes it quite easier to transform the PDEs in to ODEs. Collocation method is a numerical technique that is used to estimate the solution of BVP using polynomial and makes use of solvers with low computation memory that making it easy to implement in MATLAB code using BVP4c inbuilt function. This method is the best to solve BVP than any other numerical technique since is easy to implement.

2.3.2. Bvp4c

The bvp4c is a MATLAB solver that is based on the Collocation method that provides continuous solution with a 4th order accuracy in the interval of integration. Basically the bvp4c function solves and implements a collocation of the solution of the BVP.

2.3.3. Reduction of Higher Order Nonlinear ODEs to First Order Nonlinear ODEs

In order to reduce the governing equations, we let:

$$y_1 = f, y_2 = f^I, y_3 = f^{II}, y_4 = \omega, y_5 = \omega^I, y_6 = \phi$$

$$y_7 = \phi^I, y_1^I = f^I = y_2, y_2^I = f^{II} = y_3$$

$$y_3^I = f^{III}, y_5^I = \omega^{II}, y_7^I = \phi^{II}.$$

Thus the momentum, energy and concentration equations respectively reduces to the following:

$$y_3^I = -(m+1)\frac{\lambda r^2}{\delta} y_2 - 4y_2 - \frac{R_e}{\delta^{m+1}} y_1 y_2 + \frac{G_r(T)}{Q} y_5 + \frac{G_r(C)}{Q} y_7 - \frac{G_r(T)}{Q} y_4 - \frac{G_r(C)}{Q} y_6 \tag{31}$$

$$-y_5^I = \frac{Pr(m+1)r^2\lambda}{\delta^{m+1}} y_4 + \frac{PrEc}{r^2\delta^{m+1}} \left[4\left(y_1\right)^2 + \left(y_2\right)^2\right] + \frac{r^2\delta^{m+1}}{\left(T_w - T_\infty\right)} \frac{g_r}{c_p} Pr \tag{32}$$

$$y_7^I = \frac{-(m+1)}{\delta^{m+1}} \frac{\rho}{\mu} \lambda y_6 S_C + \frac{r^2 K_T S_C}{y_4 + N_t \delta^{m+1}} \left[y_5 y_7 - \frac{\left(y_6 + N_C(\delta^{m+1})\right)}{y_4 + N_t\delta^{m+1}} \left(y_5\right)^2\right] - \frac{r^2 K_T S_C}{y_4 + N_t\delta^{m+1}} \left(y_6 + N_C(\delta^{m+1})\right) y_5 \tag{33}$$

This is simulated by implementing the first-order nonlinear ODEs in the MATLAB software to obtain solutions.

3. Results and Discussion

3.1. *Effects of Varying Reynolds (Re) on Velocity, Temperature and Concentration Profiles*

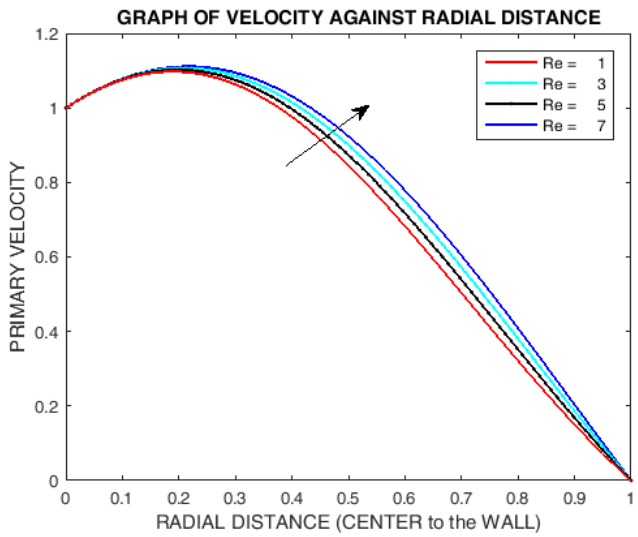

Figure 2. *Effect of varying Reynolds number on velocity profile.*

From figure 2 above, Reynold's number represents the ratio of the inertial to viscosity forces. From the velocity profile graph it is noted an increase in Reynolds number leads to an increase in velocity of the fluid flow. Increase in Reynold's number means viscous forces reduces and inertial forces become predominant. An increase in the hydrodynamic Reynolds number leads to an increase in the flow velocity due to the dominance of inertia forces over the viscous forces. Conversely, when viscous forces predominate then Reynold's number reduces and this leads to decrease in velocity profiles.

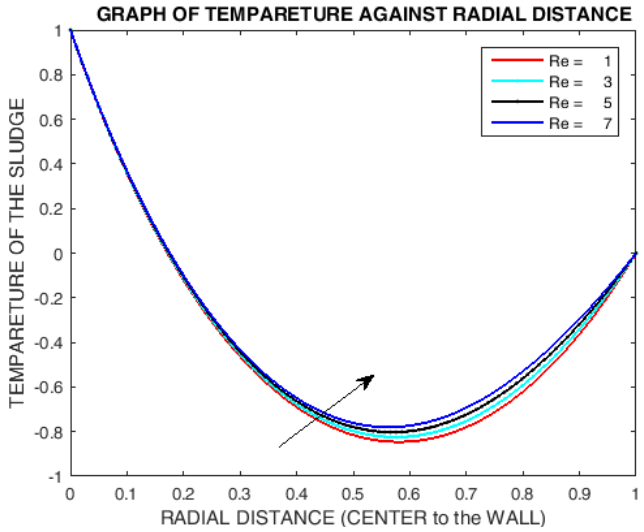

Figure 3. *Effect of varying Reynolds number on Temperature profile.*

From figure 3, when the Reynold's number increases, the temperature of the fluid flow increases. From definition of Reynold's number it shows that inertial forces become predominant and viscous forces reduces. From literature we know that when temperature is inversely proportional to the viscous forces. Thus when temperature increases the viscosity reduces and thus the cause of increase in the temperature in the flow field.

3.2. The Effects of Varying Eckert Number (Ec) on Velocity and Temperature Profiles

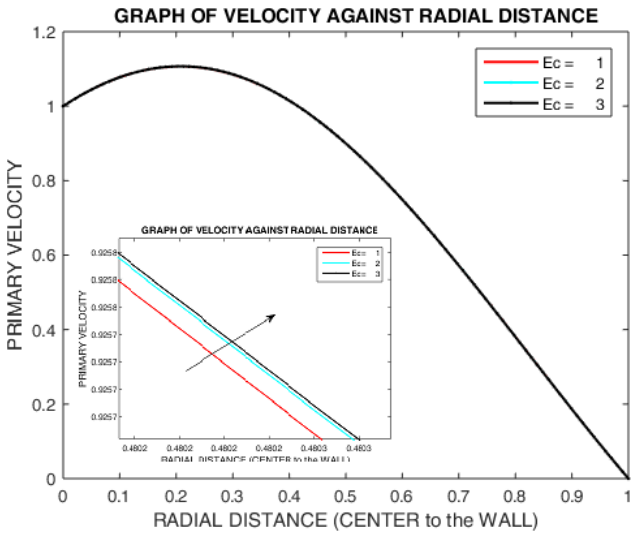

Figure 4. *Effect of varying Eckert number on velocity profile.*

From figure 4, an increase in Eckert number leads to an increase in fluid velocity. Eckert number expresses relationship of kinetic energy in the flow and the enthalpy. Basically it represent the conversion of kinetic energy into internal energy by the work which is done against the viscous fluid stress. In this, kinetic energy is predominant and thus there is a lot of bombardment of the fluid particles and hence causing a lot of vibration of the fluid particles and consequently increment of velocity of the fluid since even viscous forces are not predominant.

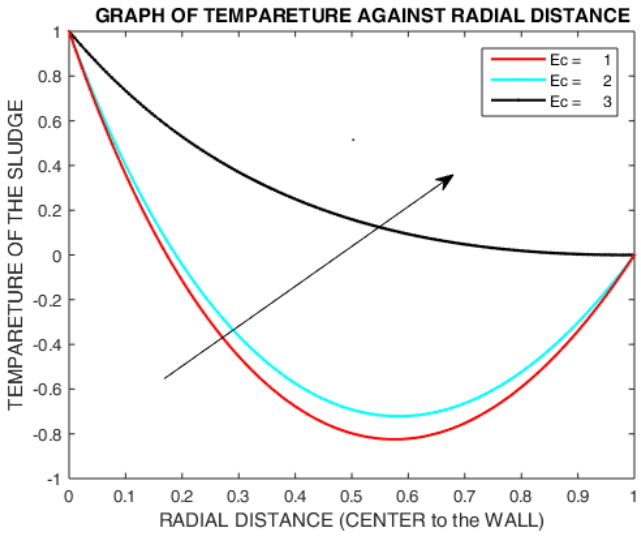

Figure 5. *Effect of varying Eckert number on temperature profile.*

From figure 5, an increase of Eckert number leads to an increment of temperature of the fluid. With kinetic energy being predominant and the velocity of fluid flow being high, the fluid particles are in constant collision and have high vibrations and this leads to high collisions of the particles. This increased collisions of the particles bring about dissipation of heat in the boundary layer region hence an increase in temperature profiles.

3.3. The Effects of Varying Schmidt Number (Sc) on Concentration Profiles

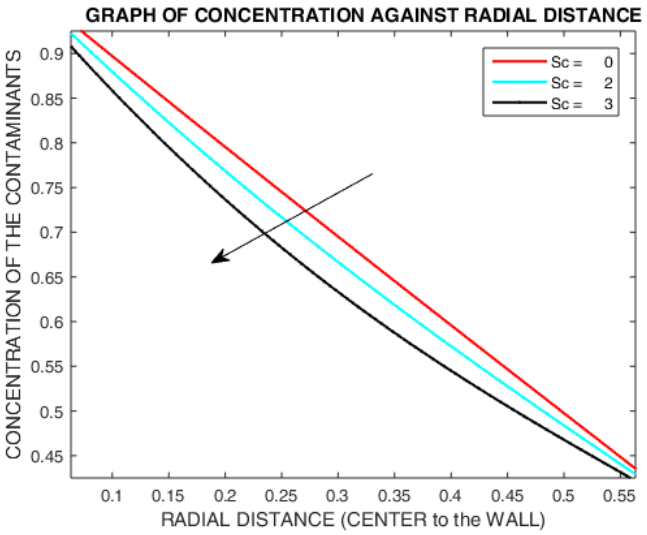

Figure 6. *Effect of varying Schmidt number on concentration profile.*

Figure 6 shows that as the Schmidt number increases, the concentration of the sludge decreases. The Schmidt number characterizes the relative importance of momentum diffusivity(kinematic viscosity) to mass diffusivity. A higher Schmidt number means that mass transfer is less efficient since mass diffusion is slowed down compared to the rate of momentum diffusion. As a result, the concentration of the sludge decreases because the sewer has a harder time transporting and mixing the sludge contaminants. If $Sc < 1$, then mass diffusion is much faster than momentum diffusion. In such cases, the substance being transported diffuses rapidly, and viscous effects are not dominant.

3.4. The Effects of Varying Concentration Ratio (Nc) on Velocity and Concentration Profiles

From figure 7, it is observed that an increase in the concentration ratio Nc results to a decrease in the concentration of sludge. By definition , increase in the concentration ratio (Nc) implies decrease in the concentration difference. This implies that the concentration of sludge is decreasing gradually towards the wall, this implies that the sludge contaminants are moving centrally. Consequently the graph of velocity profile, its noted that an increase in the concentration ratio Nc results to a increase in the velocity of sludge. This implies that the concentration difference of the sludge should not be very low.

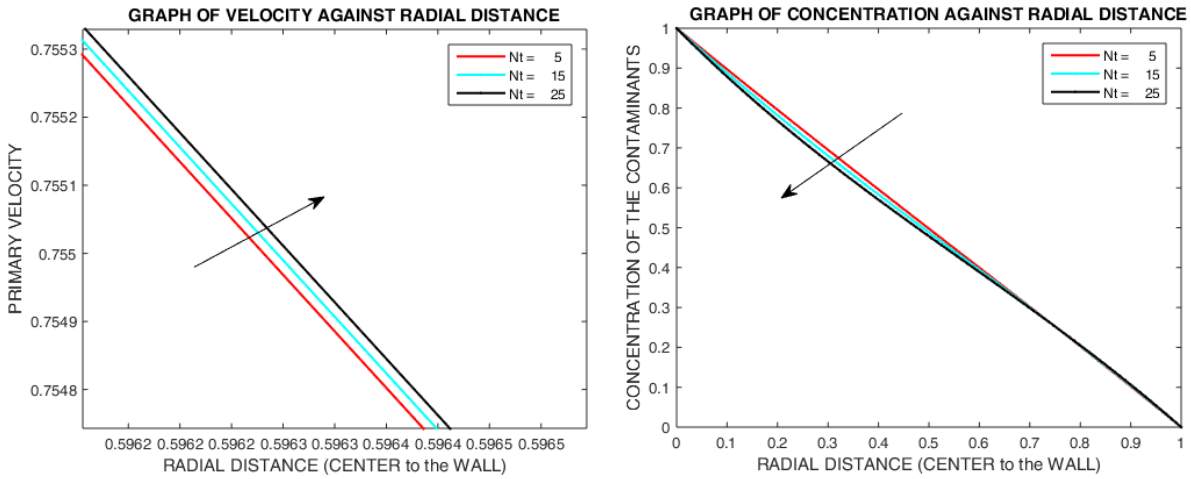

Figure 7. *Effect of varying concentration ratio on velocity and concentration profile.*

3.5. The Effects of Varying Thermophoresis Parameter (Nt) on Velocity and Concentration Profiles

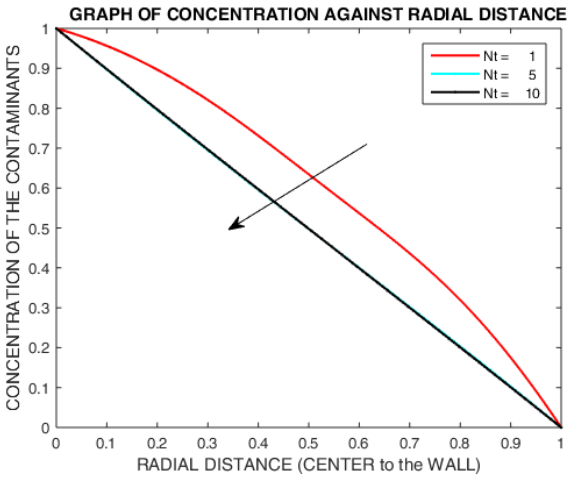

Figure 8. *Effect of varying thermophoresis parameter on velocity and concentration profile.*

From figure 8, it is observed that an increase in the thermophoresis parameter (Nt) results to a decrease in the concentration of sludge contaminants. By definition increase in the thermophoresis parameter (Nt), implies decrease in the temperature difference. This means that the wall temperature (T_∞) is increasing implying that the sludge contaminants are becoming soluble. This results to decrease in the concentration of this contaminants.

3.6. The Effects of Varying Thermal Grashof Number Gr(T) on Velocity and Temperature Profiles

From figure 9, it can be observed that an increase in the thermal Grashof number Gr(T) results to an increase in the velocity of the flow. The thermal Grashof number is defined as the ratio of buoyancy forces to viscous forces. Increase in Gr(T) implies increased forces that are driving the fluid flow. This implies increased velocity of the fluid as observed. Increase in Gr(T) also implies increase in the fluid temperature. This implies that the fluid is becoming less viscous thereby increasing its ability to flow. This results to increased velocity of the fluid.

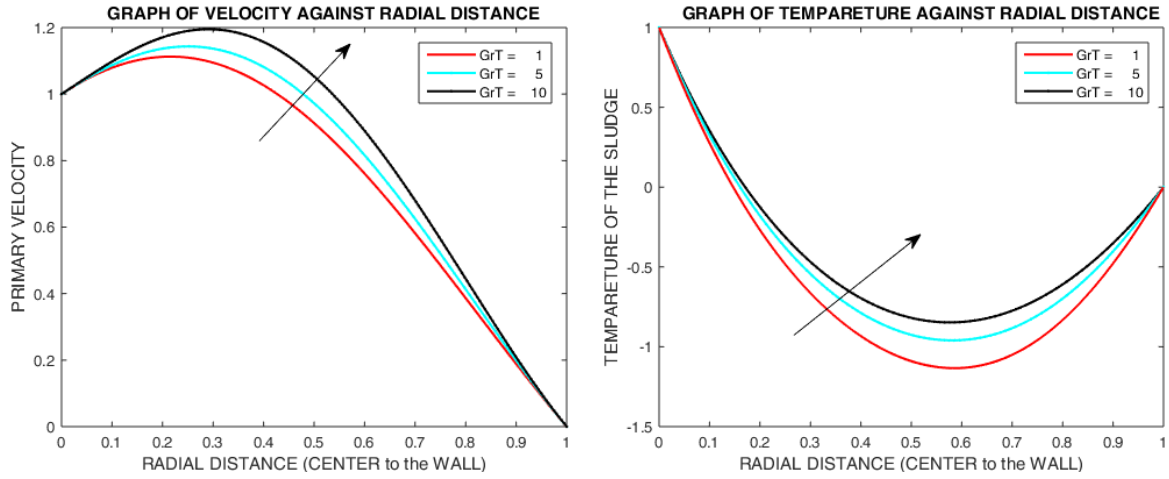

Figure 9. *Effect of varying thermal Grashof number on velocity and temperature profile.*

3.7. *The Effects of Varying Mass Grasshof Number Gr(C) on Velocity and Temperature Profiles*

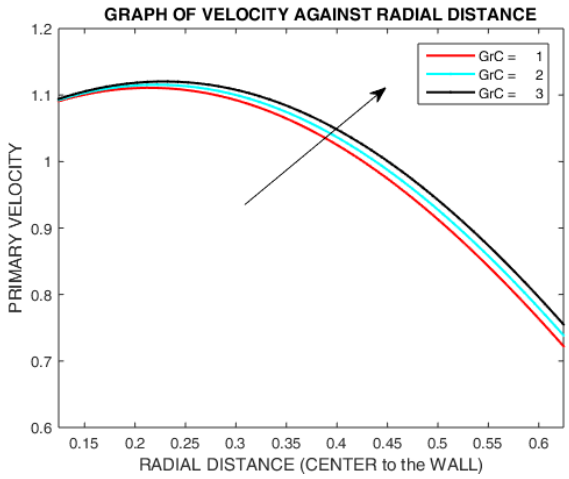

Figure 10. *Effect of varying mass Grasshof number on velocity profile.*

From figure 10, it can be observed that an increase in the mass Grasshof number Gr(C) results to an increase in the velocity of the fluid. The mass Grasshof number is defined as the ratio of buoyancy forces to viscous forces. When the viscous forces are small the velocity is high. In addition an increase in the value of mass grasshof number Gr(C) also implies an increase in the concentration difference. This means that the concentration of sludge contaminants should be optimal to maintain an optimal velocity.

4. Conclusion and Recommendation

1. Increase in Reynold's number leads to an increase in velocity and temperature profiles.
2. Increase in Eckert number leads to an increase in velocity and temperature profiles.
3. Increasing the Schmidt number leads to a decrease in the concentration profile. Increase in Sc implies decrease in mass diffusivity of the sludge contaminants which also implies decreased movement of these contaminants resulting to decreased concentration.
4. Both thermal grasshof number Gr(T) and mass grasshof number Gr(C) have an effect on the fluid velocity. Gr(T) increases the velocity of the fluid flow also Gr(C) increases the velocity of the fluid flow.
5. Increase in concentration ratio implies decrease in concentration of the sludge contaminants.
6. Increase in Nt implies decrease in the concentration of the sludge contaminants.

5. Application

This study contributes to the mathematical field through modeling maximum discharge of lateral pipes in sewage flow. Secondly, it contributes to the sewer and sanitation field of study with knowledge on the rate of heat and mass transfer between the sludge fluid and the sewer pipe. This will be significant in determining the material and or modifications to be placed on the sewer pipe in order to prevent energy loss, concentration difference hence avoiding clogging. The study also contributes in determination of the effect of concentration of the sludge contaminants in relation to velocity thereby assisting maximum discharge of lateral pipes in sewage flow.

Similar approach can also be used in the oil and gas pipelines where deposition of contaminants caused a threat of clogging of pipes. For future research the following recommendations can be implemented to extend this study.

6. Recommendations

The main user of this study are the sewerage and sanitation companies plant engineers. Recommendations to the user are as follows:

1. Integrated sewer maximizes the heat transfer rates and improves factors like cost, availability, and environmental impact.
2. Incorporating materials with specific properties in relation to heat transfer and mass transfer(due to lickages) will minimize heat loss through radiation and minimize clogging.
3. Invest more in bio digester.

The recommendations for further research are as follows:

1. Consider a turbulent flow.
2. Use of a different numerical technique.

Symbols

C	Concentration of the fluid, $[kg/m3]$
C_p	Specific heat capacity, $[jKg^{-1}K^{-1}]$
F	Body Force, [N]
g_r, g_θ, g_z	Gravitational force of the fluid, $[m/s2]$
K	Thermal conductivity, [w/mk]
p	Pressure, $[N/m^2]$
t	Time, [seconds]
T	Temperature, [K]
x, y, z	Cartesian coordinate system
r, θ, z	Cylindrical coordinate system
$q = u_r, u_\theta, u_z$	Velocity profiles, $[m/s]$
μ	Absolute viscosity, $[Kgm^{-1}s^{-1}]$
θ	Angular coordinate, [Degrees]
ρ	Fluid density, $[Kgm^{-3}]$
η	Dynamic viscosity, $[m2 = s]$
α	Thermal diffusivity, $[w = mk]$
Φ	viscous dissipation, $[N/m?]$
∇	Gradient Operator

Abbreviations

BVP	Boundary Value Problem
BVP4c	In-built solver for boundary value problems
CFD	Computational Fluid Dynanics
CSF	Continuum Surface Force
FDM	Finite Difference Method
FEM	Finite Element Method
IVP	Initial Value Problem
ODE	Ordinary Differential Equations
PDE	Partial Differential Equations

Acknowledgments

My sincere thanks, praise and honor go to The Almighty God for his unfailing love, protection, provision and sound health throughout my study period to this far. Much thanks to my supervisors, mom, dad and siblings for their guidance, counsel and support.

Author Contributions

Reuben Wambugu Mwangi: Conceptualization, Data curation, Formal Analysis, Funding acquisition, Investigation, Methodology, Project administration, Resources, Software, Visualization, Writing - original draft, Writing - review & editing

Mathew Ngugi Kinyanjui: Supervision, Validation

Phineas Roy Kiogora: Supervision, Validation

Conflicts of Interest

I declare that we have no conflicts of interest.

References

[1] J. W. Thiong'o, "Investigations of fluid flows in open rectangular and triangular channels," Journal of Applied Mathematics, vol. 17, no. 2, pp. 25-37, 2013.

[2] P. K. Marangu, E. K. Mwenda, and D. Theuri, "Modeling open channel fluid flow with trapezoidal cross section and a segment base," vol. 7, no. 1, pp. 31-38, 2016.

[3] S. M. Karimi, "Modeling fluid flow in an open rectangular channel with lateral inflow channel," Journal of Applied Mathematics, vol. 8, no. 2, pp. 31-38, 2018.

[4] M. Rubinato, S. Lee, R. Martins, and J. D. Shucksmith, "Surface to sewer flow exchange through circular inlets during urban flood conditions," Journal of Hydroinformatics, vol. 20, no. 3, pp. 564-576, 2018.

[5] D. Singh, P. Mahar, and R. Singh, "Optimal design of gravity-fed sewer lines using linear programming," Journal of The Institution of Engineers (India): Series A, vol. 100, no. 4, pp. 719-729, 2019.

[6] N. Ayub, T. Semwogerere, and R. O. Awichi, "Mathematical modelling of sewage overflow through pipe-manhole drainage sewer systems using cfd: A case of mbale city, eastern uganda," East African Journal of Engineering, vol. 2, no. 1, pp. 33-45, 2020.

[7] B. Huang, S. Wu, D. Z. Zhu, and H. E. Schulz, "Experimental study of geysers through a vent pipe connected to flowing sewers," Water Science and Technology, vol. 2017, no. 1, pp. 66-76, 2018.

[8] E. J. Noah, V. G. Masanja, H. Nampala, J. D. Lwanyaga, R. O. Awichi, and T. Semwogerere, "An application of computational fluid dynamics to optimize municipal sewage networks; a case of tororo municipality, eastern uganda.," 2020.

[9] J. Ebelait, S. Twaibu, M. Nagulama, and A. M. Keikara, "A mathematical model on linkage leakage in sewage pipes laid in a porous ground using computation fluid dynamics." East African Journal of Engineering, vol. 4, no. 1, pp. 22-32, 2021.

[10] A. C. CHIRCHIR, "The effect of two lateral inflow channels on main channel discharge," Journal of Applied Mathematics, vol. 7, no. 2, pp. 19-23, 2021.

[11] T. M. Shih, Numerical heat transfer. CRC Press, 1984.

[12] J. Polii and H. Abdurrachim, "Model development of silica scaling prediction on brine flow pipe," in Proceedings, 13th Indonesia International Geothermal Convention and Exhibition, Jakarta, Indonesia, vol. 12, 2013.

[13] G. Batchelor and C. Shen, "Thermophoretic deposition of particles in gas flowing over cold surfaces," Journal of Colloid and Interface Science, vol. 107, no. 1, pp. 21-37, 1985.

[14] J. Nagler, "Jeffery-hamel flow of non-newtonian fluid with nonlinear viscosity and wall friction," Applied Mathematics and Mechanics, vol. 38, pp. 815-830, 2017.

[15] A. Rahman, M. Alam, and M. Uddin, "Influence of magnetic field and thermophoresis on transient forced convective heat and mass transfer flow along a porous wedge with variable thermal conductive and variable thermal conductivity and variable prandtl number," Int. J. of Advances in Applied Mathematics and Mechanics, vol. 3, no. 4, pp. 49-64, 2016.